Dynamics in Supercooled Ionic Organic Liquids and Mode Coupling Theory Analysis

Jie Li, Irene Wang,† Kendall Fruchey, and Michael D. Fayer*

Department of Chemistry, Stanford University, Stanford, California 94305

Received: June 15, 2006; In Final Form: July 17, 2006

Optically heterodyne-detected optical Kerr effect experiments are applied to study the orientational dynamics of the supercooled ionic organic liquids *N*-propyl-3-methylpyridinium bis(trifluoromethylsulfonyl)imide (PMPIm) and 1-ethyl-3-methylimidazolium tosylate (EMImTOS). The orientational dynamics are complex with relaxation involving several power law decays followed by a final exponential decay. A mode coupling theory (MCT) schematic model, the Sjögren model, was able to reproduce the PMPIm data very successfully over a wide range of times from 1 ps to hundreds of ns for all temperatures studied. Over the temperature range from room temperature down to the critical temperature T_c of 231 K, the OHD-OKE signal of PMPIm is characterized by the intermediate power law $t^{-1.00\pm0.04}$ at short times, a von Schweidler power law $t^{-0.51\pm0.03}$ at intermediate times, and a highly temperature-dependent exponential (α relaxation) at long times. This form of the decay is identical to the form observed previously for a large number of organic van der Waals liquids. MCT analysis indicates that the theory can explain the experimental data very well for a range of temperatures above T_c, but as might be expected, there are some deviations from the theoretical modeling at temperatures close to T_c. For EMImTOS, the orientational dynamics were studied on the ps time scale in the deeply supercooled region near its glass transition temperature. The orientational relaxation of EMImTOS clearly displays the feature associated with the boson peak at ~2 ps, which is the first time domain evidence of the boson peak in ionic organic liquids. Overall, all the dynamical features observed earlier for organic van der Waals liquids using the same experimental technique are also observed for organic ionic liquids.

I. Introduction

Room temperature ionic liquids (RTILs) have attracted considerable attention due to their potential applications in a broad range of fields. They have good solvating properties and extremely low vapor pressures, which can make them useful solvents for reducing pollution in chemical synthesis.[1] In electrochemical devices such as fuel and solar cells[2], the advantages of RTILs arise from their thermal stability, relatively large liquid range, and the possibility of being used as both the electrolyte and the redox couple. RTILs are also being used in biocatalysis[3] and synthesis of nanostructured materials.[4] The exploration of RTILs is relatively new. A systematic study of the physical and chemical properties of this new class of liquids is therefore important for understanding and optimizing their functionality and further broadening their potential applications. Furthermore, they present a useful counter point to the properties of nonionic organic liquids for comparison.

A number of studies have recently been performed to provide information on the structure and dynamics of RTILs. Neutron[5] and X-ray[6] diffraction techniques have probed the structures of ionic liquids. Ionic conductivity and viscosity data were reported for a variety of ionic liquids with a wide range of liquid fragilities.[7] NMR spectroscopy studies have examined the molecular reorientational dynamics of an imidazolium-based ionic liquid.[8] The structures and dynamics of an ionic organic liquid have also been compared to its isoelectronic neutral binary solution at room temperature using femtosecond optical Kerr effect spectroscopy and density functional theory calculations.[9] Temperature-dependent experiments using dielectric spectroscopy[10] and neutron scattering[11,12] have been conducted to investigate the dynamics of ionic liquids in both the supercooled liquid and glassy amorphous states. Several single-particle time correlation functions were calculated using molecular dynamics simulation to characterize distinct dynamical processes in ionic liquids.[13] Despite the exponential growth of the research activities carried out on RTILs, further studies on the dynamics of these substances are required to obtain a fundamental understanding of their chemical reactivity and transport properties on a molecular level.

In this work, we study the orientational dynamics of supercooled organic ionic liquids over a broad range of times and temperatures using optically heterodyne-detected optical Kerr effect (OHD-OKE) spectroscopy.[14−16] The glassy dynamics of organic molecular liquids have been studied extensively using time domain OHD-OKE experiments[15,17−22] and frequency domain light scattering experiments.[23−25] The experimental results have been discussed in the framework of mode coupling theory (MCT), usually through the application of schematic mode coupling theory models.[18,25−27] Compared to molecular liquids, ionic liquids are distinct because they have long-range Coulomb interactions between ions. It is interesting to investigate whether the nature of the intermolecular interactions affects the structural relaxation of RTILs in the supercooled state as the glass transition temperature is approached.

In the full MCT, the interaction potential enters the equations through the static structure factor.[27] However, schematic MCT, which makes the calculations of observables tractable, does not explicitly contain the form of the intermolecular potential. The schematic MCT equations (see below) calculate an orientational

* To whom correspondence should be addressed. E-mail: fayer@stanford.edu.

† Permanent address: Université Claude Bernard Lyon 1, 69622 Villeurbanne, France.

10.1021/jp0637476 CCC: $33.50
Published on Web 08/16/2006

correlation function coupled to a density correlation function.[18,26] These correlation functions are for damped oscillators with memory functions. The memory function describes the caging of the position and orientation degrees of freedom of molecules by the surrounding molecules. Full randomization of the system requires relaxation of the cage. Cage relaxation slows as the temperature is lowered. The general structure of the schematic MCT equations predicts certain time dependent forms for the observables[18,26] as well as temperature-dependent scaling relations.[28] Examining temperature-dependent experimental data with schematic MCT tests the applicability of the schematic model and yields a set of parameters that can be compared from one system to another.

Analyzing experimental data taken on RTILs with schematic MCT and comparing the results to van der Waals liquids will bring out unique aspects of the dynamics of supercooled RTILs if any exist. Extensive OHD-OKE experiments have been conducted on a large number of organic molecular liquids.[15,17−22] The experiments and data analysis have demonstrated certain features of the time evolution of these systems that are universal. Examples include a temperature independent, nearly logarithmic decay of the orientational correlation function at intermediate time scales[19,26,29] and a ps time scale boson peak which develops as the glass transition is approached from above.[18,20,22] The question arises as to whether such features are also found in RTILs.

A previous temperature-dependent OHD-OKE was applied to an imidazolium-based ionic liquid.[30] However, the experiments could only be conducted into the weakly supercooled region, ∼40 K above the MCT critical temperature T_c.[27] Experiments at lower temperatures were prevented by crystallization of the sample. In this paper, we report OHD-OKE data on a typical ionic organic liquid, *N*-propyl-3-methylpyridinium bis(trifluoromethylsulfonyl)imide (PMPIm), over a wide range of temperatures from room temperature to MCT critical temperature T_c. The data will be compared to the results from molecular liquids and analyzed in the framework of MCT.[26,27] We will also present OHD-OKE data on a different ionic liquid, 1-ethyl-3-methylimidazolium tosylate (EMImTOS) near its glass transition temperature T_g (201 K). In a deeply supercooled state, this material clearly exhibits the feature of the boson peak at temperatures of 3−27 K above T_g. Overall, all the dynamical features observed earlier for organic molecular liquids using the identical experimental technique are also observed for organic ionic liquids.

II. Experimental Procedures

OHD-OKE spectroscopy[14−16] was used to study the orientational dynamics of two organic ionic liquids, PMPIm and EMImTOS. The OHD-OKE experiment measures the time derivative of the polarizability−polarizability correlation function, which is directly related to the data obtained from depolarized light scattering experiments by Fourier transform.[31−34] The polarizability−polarizability correlation function is essentially the second Legendre polynomial orientational correlation function except at short time (less than a few ps) where collision induced effects (density fluctuations) can also contribute to the decay.[32−35] In the experiments, a pump pulse creates an optical anisotropy and a probe pulse is used to heterodyne detect its decay at variable time delays. To observe the full range of liquid dynamics, at each temperature several sets of experiments were performed with different pulse lengths and delays. For times t < 30 ns, a 5 kHz mode-locked Ti:Sapphire laser/regenerative amplifier system was used (λ = 800 nm) for both pump and probe. The pulse length was varied by from 75 fs to 100 ps as the time scale of the measurement increased to improve the signal-to-noise ratio. For longer times, a CW diode laser was used as the probe, and a fast digitizer (1 ns per point) recorded the data. The scans taken over various time ranges overlapped substantially, permitting the data sets to be merged by adjusting only their relative amplitudes. The details of the experimental setup can be found in previously published work.[21,36]

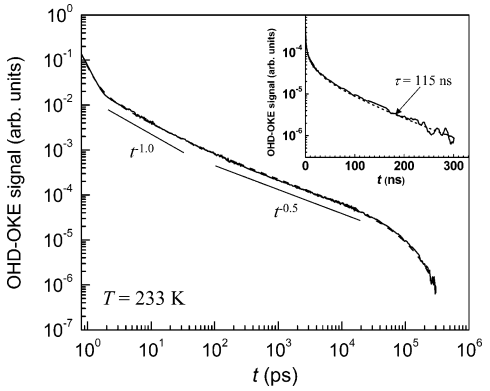

Figure 1. OHD-OKE data for PMPIm at T = 233 K on logarithmic scale. The dashed line through the data is the fit using eq 1. The two straight lines are aids to the eyes indicating the intermediate power law and von Schweidler power law. (Inset) Exponential decay (the α relaxation) at long times on a semilogarithmic scale.

PMPIm was purchased from Strem Chemicals, Inc., and EMImTOS was purchased from Aldrich. Both samples were used without further purification other than filtration through 0.1 mm disk filters to remove dust and reduce light scattering. The samples were sealed under vacuum into glass cuvettes of optical path length = 1 cm. The cuvettes were held in a liquid nitrogen constant flow cryostat where the temperature was controlled to ±0.1 K. The glass transition temperatures of both samples were measured using Q100 differential scanning calorimeter from TA Instruments, Inc. PMPIm shows a glass transition at 186 K and EMImTOS shows a glass transition at 201 K in their heating curves with heating rate = 15 K/min.

III. Results and Discussion

Using OHD-OKE experiments, the orientation dynamics of PMPIm were studied over a broad temperature range from the mode coupling theory critical temperature T_c to ∼60 K above it. Figure 1 is an example of the data taken at T = 233 K. The shape of the decay curve is very similar to those that have been observed earlier for supercooled molecular liquids.[19] A phenomenological fitting function was found to describe the OHD-OKE data of molecular liquids very well.[19] This function is used to perform global fits to the data and extract parameters. In this work the PMPIm data is analyzed using a very similar fitting function and an MCT analysis is given below. The fitting function is

$$F(t) = [at^{-s} + pt^{-z} + dt^{b-1}] \exp(-t/\tau_\alpha) \qquad (1)$$

If the at^{-s} term is excluded, the rest of the function is identical to the phenomenological fitting function that has been used previously for van der Waals liquids.[19,37] The term at^{-s} is added to account for the decay at the shortest time scale from sub ps to a few ps. In MCT descriptions of supercooled liquids, the very short time portion of the decay is a power law called the fast β process.[20,27] Following the shortest time scale decay is the intermediate power law pt^{-z}.[19,29,37] The decay after the

intermediate power law is another power law dt^{b-1} called von Schweidler power law, which then crosses over to the final exponential decay, the α relaxation. [20,27,37] For supercooled van der Waals liquids, the exponents z and b are found to be temperature independent. [19,29,37] The exponential α relaxation, however, is highly temperature dependent, with the time constant τ_α increasing dramatically as the glass transition is approached from above.[19]

Equation 1 is an empirical function that provides a convenient and simple method to analyze and compare data for different liquids.[19,37] The power laws are chosen because they provide high-quality fits with minimum number of parameters and have some connection to MCT, although not a formal connection. The existence of the power laws has been established in the framework of MCT and confirmed in other experiments. The critical power law (shortest time scale power law) and the von Schweidler power law (longest time scale power law) are the leading order terms in the MCT asymptotic solutions.[38,39] Prior to the identification of the intermediate power law, a superposition of the critical decay and the von Schweilder power law was used as a simple interpolation formula to fit susceptibility spectra around the minimum.[25,40−42] The intermediate power law is the time-domain equivalent of the near constant loss observed in susceptibility spectrum.[43] The two-correlator schematic MCT model with the orientation coupled to density fluctuations is able to reproduce the decay in general including the intermediate power law.[26] Although the additivity of the three power law decays in the empirical equation is not specified in MCT, eq 1 is a useful MCT-like expression that contains the features found in both the data and the MCT calculations and facilitates a global fit to the data, permitting comparison of parameters among samples.

The data shown in Figure 1 have the components of eq 1. The calculated curve using eq 1 is displayed as the dashed curve. Over the full time window from 0.8 ps to ∼300 ns, the calculated curve follows the experimental data very well. The fitting results for the data at 233 K are $s = 3.83$, $z = 1.03$, $b = 0.50$, and $\tau_\alpha = 115$ ns. A global fit is used to account for one type of decay giving way to the next as time is increased. In the double-logarithmic representation of Figure 1, two straight lines are drawn as aides to eye indicating the two power laws $t^{-1.0}$ and $t^{-0.5}$. The intermediate power law $t^{-1.0}$ spans a limited time interval due to the onset of the von Schweidler power law $t^{-0.5}$. The von Schweidler power law spans more than two decades of time from 100 ps to ∼20 ns. The inset of Figure 1 is a semilog plot showing the exponential decay (the α relaxation) at long times. The exponential decay appears as a straight line after ∼60 ns.

Figure 2 displays the OKE data and calculations using eq 1 for the range of temperatures studied. From the top to the bottom, the curves are arranged in the order of increasing temperatures. The curves have been off-set along the vertical axis for clarity of presentation. The lowest temperature data span the longest time window because the final complete α structural relaxation slows down as the temperature is decreased. The functional form of OHD-OKE decay curves does not change when the temperature is varied, but the numerical values of some of the fitting parameters change with temperature. The temperature dependence of the three power law exponents are displayed in Figure 3a,b. The short time power law exponent s (Figure 3a) increases as the temperature decreases. Because the short time power law t^{-s} decays fast and is observable over a limited time range, it is difficult to determine its exact functional form.

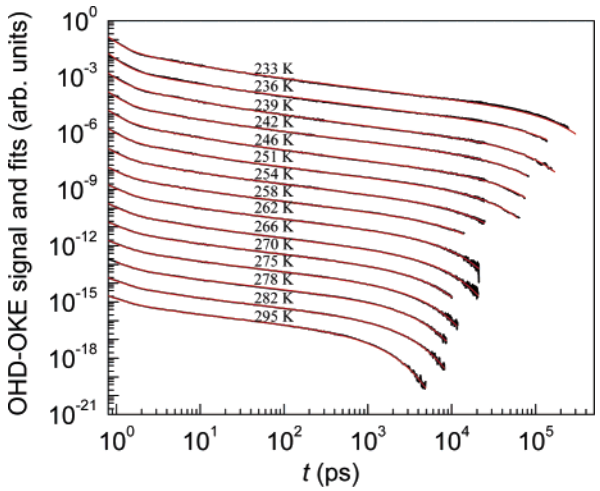

Figure 2. Temperature-dependent OHD-OKE PMPIm data on a log plot. The data sets have been off-set along the vertical axis for clarity of presentation. Fits to the data using eq 1 are shown (red lines).

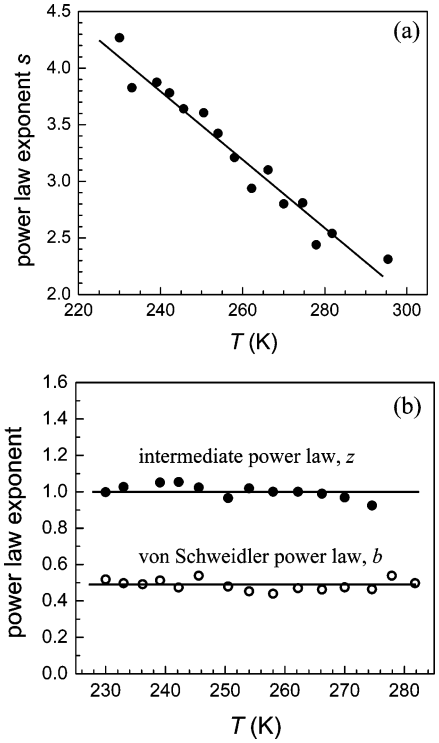

Figure 3. Results of the fits to the PMPIm data in Figure 2 using eq 1. (a) Temperature dependence of the short time power law (fast β process) exponent s. (b) Temperature dependence of the intermediate power law exponent z and von Schweidler power law exponent b. z and b are found to be independent of T. The lines through the points show the average values.

MCT predicts a power law in this time range. What is clear is that the short time dynamics are temperature dependent.

The intermediate power law exponent z and the von Schweidler power law exponent b do not depend on temperature within experimental errors (Figure 3b). The value for z is 1.00 ± 0.04. Previously OHD-OKE experiments on five nonionic aromatic liquids observed T-independent intermediate power law decays with the exponents in the range of 0.79−1.0.[19] Earlier studies on an imidazolium-based ionic liquid in weakly supercooled state revealed an intermediate power law $t^{-1.02\pm0.05}$.[30] OHD-OKE experiment measures the time derivative of orientational correlation function and is directly related to frequency domain experiments by Fourier transform. An intermediate

power law t^{-z} with $z \approx 1$ corresponds to a logarithmic decay or very close to a logarithmic decay in the correlation function, which is the exact equivalent of a near constant loss in the susceptibility spectrum.[37,43−46] With the results from five aromatic van der Waals liquids and two organic ionic liquids, the nearly logarithmic decay of the intermediate time scale has been demonstrated to be a universal feature of fragile glass-forming liquids. The von Schweidler power law exponent b is 0.49 ± 0.03 for PMPIm as shown in Figure 3b. The b value for the imidazolium-based ionic liquid was 0.87 ± 0.06.[30] The b values from the ionic liquid studied here falls outside the range 0.73−0.85 reported[37] previously for nonionic aromatic liquids and for the imidazolium ionic liquid. On the basis of current information from OHD-OKE studies on organic molecular and ionic liquids, the presence of the intermediate power law and von Schweidler power law and their temperature dependence do not change with the nature of the liquid. The Coulomb interactions present in the RTILs do not appear to influence the fundamental nature of the dynamics. With the exception of the von Schweidler power law exponent for PMPIm studied here, the numerical values of the two power law exponents have no systematic difference between these two types of liquids as well. The $b = 0.5$ found for PMPIm may also all fall within the "normal" range if the study of more compounds expands the range.

MCT provides a framework to quantify the dynamics of supercooled liquids. It predicts certain scaling relations[28] for the supercooled liquids as they approach the MCT critical temperature T_c. T_c is called the "ideal" glass transition temperature because in standard MCT, the α-relaxation is predicted to diverge at T_c, becoming infinitely slow. The cessation of complete structural relaxation predicted by MCT to occur at T_c, that is, the liquid becomes nonergodic, was thought to signal the glass transition. However, experimentally the α-relaxation time does not become infinitely slow at T_c and continues to increase below T_c. The experimental glass transition temperature T_g is usually 15−20% below T_c. Previously reported OHD-OKE data on several supercooled organic molecular liquids obey the MCT scaling relations at temperatures above T_c.[19] As an initial test of MCT in ionic liquid systems, the standard MCT scaling law analysis was performed on PMPIm. The MCT scaling relation for the α-relaxation time constant,τ_α, scales with temperature as[28]

$$\tau_\alpha \propto (T - T_c)^{-\gamma} \text{ or } \tau_\alpha{}^{-1/\gamma} \propto T - T_c \qquad (2)$$

with

$$\gamma = (a + b)/2ab \qquad (3)$$

and a and b are MCT parameters, which are related to each other via

$$\Gamma^2(1 - a)/\Gamma(1 - 2a) = \Gamma^2(1 + b)/\Gamma(1 + 2b) \qquad (4)$$

where Γ is the gamma function and b is the von Schweidler power law exponent, which is obtained experimentally (see Figure 3b). The von Schweidler power law amplitude(eq 1) scales with temperature as,[28]

$$d \propto (T - T_c)^{\delta} \text{ or } d^{1/\delta} \propto T - T_c \qquad (5)$$

with

$$\delta = (a + b)/2a \qquad (6)$$

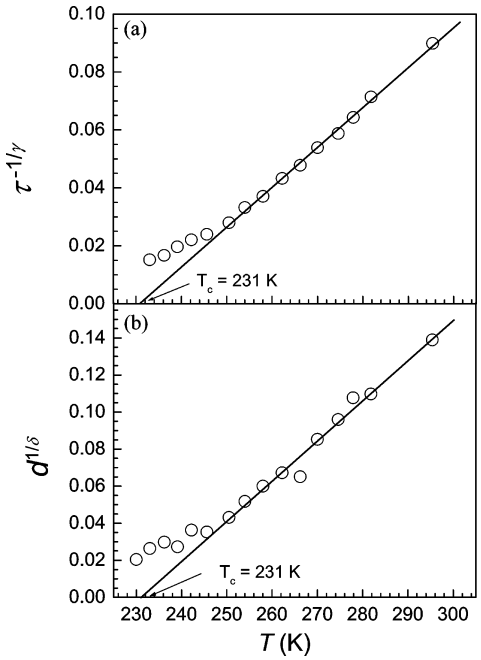

Figure 4. Scaling plots for (a) the exponential decay time constant τ_α (plotted as $\tau_\alpha{}^{-1/\gamma}$) and (b) the amplitude of the von Schweidler power law, d (plotted as $d^{1/\delta}$). The straight lines are the fits to MCT scaling relations (see eqs 2−6). The points close to T_c are omitted from the fits (see text). Both fits yield $T_c = 231$ K.

Using the value 0.49 for b determined from the fits, a is found to be 0.28 from eq 4. Then γ and δ are 2.79 and 1.36, respectively, using eqs 3 and 6.

Figure 4a displays the rectification diagram for τ_α. The experimental data points (○) over a significant temperature range fall on a line, indicating the validity of MCT scaling relationship. The solid line is a linear fit to eq 2 using T_c and a proportionality factor as adjustable parameters. The extrapolation of the calculated line to its intersection with the abscissa yields $T_c =$ 231 K. The data points close to the critical temperature T_c, however, show deviations from the line. Simple MCT predicts that the long time scale α-exponential decay becomes infinitely slow at T_c, which disagrees with experimental observations. This discrepancy is well-known and may be corrected by adding an activated hopping mechanism below the ideal glass transition temperature T_c.[47] In this context, the data points at the lowest five temperatures are simply excluded from the fit.

To compare the von Schweidler power law amplitudes at different temperatures, a normalization is used to correct for laser intensity drift and the temperature dependence of the sample density. At $t = 0$, the OHD-OKE signal is overwhelmingly dominated by the instantaneous electronic response of sample. Because both the density changes caused by temperature variation and any laser intensity drift have essentially the same effect on the nuclear part and the electronic part of OHD-OKE signals, the OHD-OKE orientational relaxation data were normalized to the instantaneous electronic response at $t = 0$. After applying the normalization, the temperature dependence of the von Schweidler power law amplitude d (plotted as $d^{1/\delta}$) is shown in Figure 4b. A linear fit using eq 5 is shown as the solid line. Again, the data points at the lowest five temperatures are not considered when performing the fit. T_c is found to be 231 K, consistent with the result determined from τ_α. The ratio $T_g/T_c = 0.81$. For comparison, the ratios for 2-biphenyl phenol, ortho-terphenyl, salol, dibutylphthalate, benzophenone, and acetylsalicylic acid are 0.82, 0.83, 0.85, 0.79, 0.85, and 0.87,

respectively. Therefore, the ratio of the RTIL falls within the range of the ratios for common molecular liquids.

Recently, a MCT schematic model, the Sjögren model,[48] was solved numerically and compared to OKE data of several supercooled molecular liquids.[18,26] This model was able to accurately reproduce temperature-dependent data for organic liquids down to T_c, and it was also able to reproduce the appearance of the boson peak at and below T_c.[18] Here, we present a detailed schematic MCT analysis on the ionic liquid PMPIm using the same model. The Sjögren model involves two correlation functions, one for density and one for the experimental observable, in this case, the orientation (polarizability−polarizability) correlation function. The equation for the density correlation function has the form of a damped harmonic oscillator with a memory term. The memory term accounts for the caging effects. The density relaxation is complicated by correlations in the local density that inhibits relaxation. This caging effect becomes more pronounced as the temperature is lowered. The memory function uses an F_{12} model, that is it contains a term that is linear in the correlation function and a term that is quadratic in the correlation function (see eq 8 below).[27] The experimental observable correlation function is coupled to the density correlator, which possesses the relevant singular behavior as the mode coupling transition is approached. In the following, ϕ_1 is the density correlator and ϕ_2 is the orientation correlator. Coupling the orientational correlation function to the density correlation function builds memory effects into the orientational relaxation. The MCT F_{12} model equations for the density correlator and the coupled orientation correlator are given by

$$\ddot{\phi}_i(t) = -\Omega_i^2\phi_i(t) - \mu_i\dot{\phi}_i(t) - \Omega_i^2\int_0^t \mathrm{d}t' m_i(t-t')\dot{\phi}_i(t') \qquad i = 1,2 \quad (7)$$

where $\Omega_{1,2}$ are the characteristic frequencies and $\mu_{1,2}$ are the damping constants for the density and orientation correlators, respectively. The memory kernels are given by

$$m_1(t) = v_1\phi_1(t) + v_2\phi_1(t)^2 \quad (8)$$

$$m_2(t) = k\phi_2(t)\phi_1(t) \quad (9)$$

where v_1 and v_2 are the coupling constants in the density memory kernel and k is the translation-rotation coupling constant. The initial conditions are $\phi_{1,2}(0) = 1$ and $\dot{\phi}_{1,2}(0) = 0$.

There are a large number of parameters that go into the calculations. For supercooled liquids, the characteristic frequencies are on the order of THz.[16] To reduce the complexity, we assume that $\Omega_{1,2}$ are independent of temperature. This is reasonable since $\Omega_{1,2}$ are expected to show weak temperature dependence and the experimental temperature range is not wide. We chose $\Omega_1 = 1$ THz, $\Omega_2 = 0.5$ THz to be consistent with the values used earlier for organic liquids.[18] It was found previously that the nature of the results is not sensitive to the choice of Ω_1 and Ω_2. Varying Ω_1 and Ω_2 changes the values of some of the other parameters but does not change the temperature-dependent trends. In the initial fits of the data, all other parameters were allowed to vary. The theoretical curves for comparison to the experiments were calculated as the time derivative of $\phi_2(t)$ obtained from the solutions of eqs 7−9. A downhill simplex algorithm was used to fit the experimental data. In the preliminary fits, it was found that the parameters v_1 in the density memory kernel and the density damping constant μ_1 were virtually independent of temperature. Therefore, we fixed the values of v_1 and μ_1 to be 0.97 and 5.5, respectively, which were determined by the average values from the preliminary fits. The temperature dependence of other parameters v_2, μ_2, and κ do not change whether v_1 and μ_1 are fixed or not.

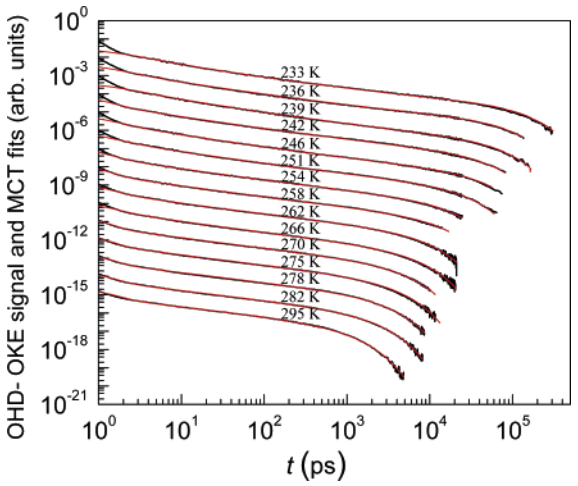

Figure 5. Temperature-dependent PMPIm OHD-OKE data and the MCT calculated curves (red) using the solutions to eqs 7−9 on a log plot. The curves have been off-set along the vertical axis for clarity of presentation. The agreement between the schematic MCT calculations and the data are excellent except at shortest times (<2 ps) at the lowest few temperatures.

Figure 5 displays the results of the fits obtained by fixing Ω_1, Ω_2, v_1, and μ_1 to the values given above and adjusting v_2, μ_2, and κ at each temperature. The curves have been off-set along the vertical axis for clarity of presentation. The fits start from 1 ps. Data at even shorter times are not considered because they are obscured by the electronic response of the sample, which is so strong that even with short pulses, it overwhelms the nuclear contributions to the signal. The electronic polarizability signal becomes negligible for $t \geq 1$ ps. Over a wide time window, ranging from ~1 ps to hundreds of ns, and over a wide range of temperatures above T_c, the Sjögren model reproduces the dynamics of ionic liquids very successfully except for the very shortest times at the lowest temperatures. At the lowest temperatures, for $t < 2$ ps, the calculations do not reproduce the initial steep decay, the fast β process. The quality of the fits is as good as those demonstrated earlier for organic van der Waals liquids.[18,26] In the van der Waals liquids, data for $t < 2$ ps were not considered.

Figure 6 displays the F_{12} phase diagram[27] formed by v_1 and v_2, the coupling constants of the density memory kernel. The F_{12} phase space is split by the liquid-ideal glass transition lines (dashed line for type-*A* transition and solid line for type-*B* transition) into two regions with lower left corresponding to the ergodic liquid state and the upper right corresponding to the nonergodic ideal glass state. The open circles are the results of the fits in Figure 5. They form a trajectory which illustrates the evolution of the glassy dynamics in the system as it is cooled toward the ideal glass transition. Extrapolation of the trajectory crosses the type-*B* transition line at the liquid-ideal glass transition point (v_1^c,v_2^c), suggesting that an ergodic-nonergodic type-*B* transition would occur if the system is cooled further. This is consistent with the belief that a type-*B* transition is associated with structural glass transitions. A type B transition is a discontinuous phase transition at which the nonergodicity parameter (the long time limit of the density correlation function) jumps from zero to a nontrivial value, indicating the freezing of the density fluctuations into the glassy state. The critical point (v_1^c, v_2^c) is related to the von Schweidler power law

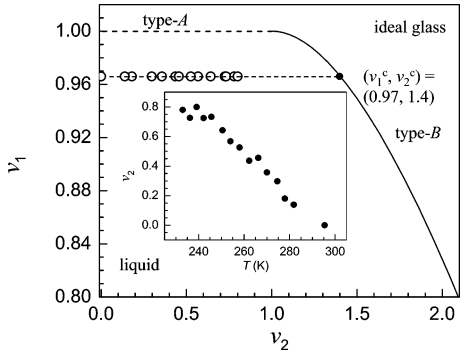

Figure 6. Trajectory of the MCT coefficients v_1 and v_2 (equations 7 and 8) on the schematic F_{12} phase diagram. (○) Values obtained from fits to the data shown in Figure 5. The extrapolation of the trajectory (the dashed line) intersects with the liquid-glass transition line (the solid curve) at the critical point (●). (Inset) Temperature dependence of the coefficient v_2.

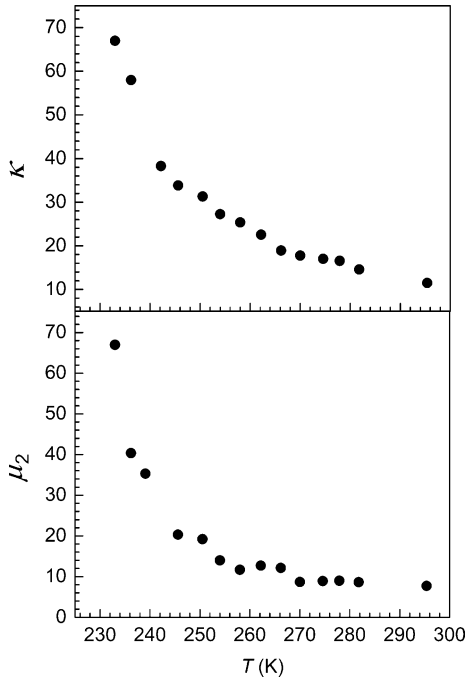

Figure 7. Temperature dependence of the translation-rotation coupling κ and the orientational damping constant μ_2. The values are obtained from the fits in Figure 5.

exponent b:[26]

$$\lambda = \Gamma^2(1+b)/\Gamma(1+2b)$$
$$v_1^c = (2\lambda - 1)/\lambda^2 \qquad (10)$$
$$v_2^c = 1/\lambda^2$$

For PMPIm, b (equation 1) is 0.49, from which (v_1^c, v_2^c) is calculated to be (0.93, 1.59), which is close to the real crossing point (0.97, 1.4) (●) on the phase diagram obtained from fitting the data with the schematic MCT model. The inset of Figure 6 shows the variation of v_2 with changes of the temperature. v_2 increases with decreasing T, showing that the memory effect (caging) increases as the temperature is lowered.

The temperature dependences of the translation-rotation coupling constant κ, and the orientation damping constant μ_2 are shown in Figure 7. Both κ and μ_2 increase rapidly as temperature decreases. The growth of coupling between translational and rotational degrees of freedom seems to be a universal characteristic found in several different liquid systems. For nematic liquid crystals, a modified MCT schematic model was used to describe the orientational dynamics of nematogens in the isotropic phase.[49] κ was found to increase with decreasing temperature and diverged at the nematic−isotropic phase transition. For organic van der Waals liquids, the increase in κ is responsible for the appearance of the boson peak as the temperature approaches and drops below T_c.[18] This strong translation−rotation coupling is also responsible for the nearly logarithmic decay (the intermediate power law) observed in OHD-OKE experiments for organic van der Waals liquids[26] and the ionic liquid PMPIm studied here. Although the relevance of κ to the liquid-glass transition is not contained in MCT, the increase in κ is essential to reproduce the variation of the data with decreasing T. Here, μ_1 is held constant. This is in accord with the result for molecular liquids above T_c. In contrast, μ_2 is relatively constant at the higher temperatures and then increases at the lowest temperatures as T_c is approached. In studies of molecular liquids, the same type of MCT fits were performed, but it was possible to hold μ_2 constant and reproduce the data, including the boson peak (see below).[18] However, in using a modified schematic MCT model to fit equivalent data for nematogens in the isotropic phase, μ_2 is highly temperature dependent.[49] It is unclear if the temperature dependence of μ_2 shown in Figure 7 reflects a significant difference of RTIL from molecular liquids.

To this point, we have demonstrated that PMPIm, a typical organic ionic liquid, exhibits several dynamical features (the intermediate power law, von Schweidler power law, and exponential α relaxation) that have been observed previously on molecular glass-forming liquids. The general form of the features, that is, the power law exponents, temperature dependences, accordance with MCT scaling relations, and the ratio T_g/T_c are essentially indistinguishable from the results found for van der Waals organic liquids. Another feature associated with supercooled liquids as the temperature approaches T_g is the boson peak. It has been observed in previous OHD-OKE experiments on several supercooled molecular liquids as a highly damped oscillatory feature appearing around 1−2 ps at temperatures below T_c.[18,20,22] It has also been observed as a bump at THz frequencies in Raman and neutron scattering spectra and specific heat and thermal conductivity anomalies in many other disordered systems including silica glasses,[50] alcohol glasses, [51,52] and metallic glasses.[53] The boson peak is described as an excess of low energy modes in the vibrational density of states. In the time domain, as the caging becomes very strong with the time of relaxation of the cage greater than the inverse frequency for oscillation in an essentially fixed potential, an oscillatory component appears in the dynamics.

Because the boson peak appears at temperatures below T_c, it was not possible to look for its appearance in PMPIm because the samples crystallized. Therefore, another RTIL, EMImTOS, was studied. EMImTOS could be cooled well below its T_c. Figure 8 shows the EMImTOS data on the ps time scale at several temperatures. As T decreases, a full cycle of oscillation starts to develop around 2 ps and the depth of modulation continues to increase. The signal actually goes negative at the lowest temperature, which is only 3 K above the calorimetric glass transition temperature. This is possible because the signal is heterodyne detected. The oscillation has a period of ∼2 ps estimated from the separation between its neighboring maximum and minimum. This highly damped oscillatory feature corresponds to the boson peak. Very recently, evidence of the boson peak was reported on an imidazolium-based ionic liquid using

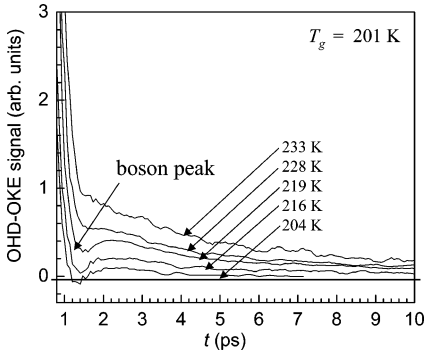

Figure 8. OHD-OKEdata for EMImTOS at short times, 0.8−10 ps. As the temperature decreases, an oscillatory component, the boson peak, develops.

specific heat measurements.[54] Here, we can see directly the time domain signature of the boson peak in an RTIL.

IV. Concluding Remarks

We have presented temperature-dependent OHD-OKE data on the supercooled organic ionic liquids PMPIm and EMImTOS. From MCT critical temperature T_c to ~60 K above it, the intermediate power law $t^{-1.00\pm0.04}$ and von Schweidler power law $t^{-0.51\pm0.03}$ are observed for PMPIm at short to intermediate times, and the long time scale decay is the exponential α relaxation. The temperature dependent data for PMPIm are completely consistent with many organic van der Waals liquids that have been studied previously using the same experimental technique. The data obey MCT scaling relations over a wide range of temperatures above T_c, although some deviations from the theory appear as T approaches T_c. The MCT critical temperature T_c is determined to be 231 K for PMPIm. The ratio of $T_g/T_c = 0.81$. The ratio falls into the range that has been reported earlier on fragile van der Waals liquids. The PMPIm data were also compared to a MCT schematic model, the Sjögren model, which has been demonstrated previously to be capable of successfully reproducing the OHD-OKE data of several organic van der Waals liquids. In this work the Sjögren model was able to describe the PMPIm data equally well. The OHD-OKE data for EMImTOS exhibits the boson peak at ~2 ps for temperatures close to T_g. All these features observed for these RTILs are typical of fragile van der Waals glass-forming liquids, which is consistent with previous OKE studies on a different organic ionic liquid.[30]

Recently, heat capacity measurements on an imidazolium-based ionic liquid suggest that it is a fragile and disordered system with thermodynamic properties that are similar to molecular glass-forming liquids.[54] Dynamics of a room-temperature ionic liquid were also compared to its analogous isoelectronic binary solution at room temperature.[9] It was found that the ionic liquid has larger density and viscosity than its neutral pair due to the stronger interactions between ions and the reorientational relaxation time constants of these two systems scale with their viscosities indicating hydrodynamic theory is relevant for the diffusive dynamics in ionic liquids.[9]

Temperature-dependent OHD-OKE experiments provide detailed information on the coupled translation-orientational dynamics in liquids over a broad range of times from < ps to hundreds of ns and tens of μs in some instances. Current information from OHD-OKE experiments indicates that the dynamics of RTILs and molecular liquids display universal features over a wide range of temperatures above mode coupling theory critical temperature T_c and behave similarly as T_g is approached. Other experiments performed on RTILs also support the similarity of RTILs and organic molecular liquids.[9,54] The interesting question is should we be surprised at these results? RTILs are binary liquids with Coulomb interactions between the cations and anions. This is in contrast to organic molecular liquids that are generally relatively nonpolar and interact mainly through van der Waals interactions. This basic difference in the nature of the interactions does not appear to play a role in producing distinct thermodynamic or dynamic characteristics of the bulk liquids.

Acknowledgment. This work was supported by the National Science Foundation (DMR-0332692).

References and Notes

(1) *Ionic Liquids: Industrial Applications to Green Chemistry*; Rogers, R. D., Seddon, K. R., Eds.; American Chemical Society: Washington, DC, 2002.
(2) Wang, P.; Zakeeruddin, S. M.; Moser, J. E.; Gratzel, M. *J. Phys. Chem. B* **2003**, *107*, 13280.
(3) van Rantwijk, F.; Madeira Lau, R.; Sheldon, R. A. *Trends Biotechnol.* **2003**, *21*, 131.
(4) Chen, L. J.; Zhang, S. M.; Wu, Z. S.; Zhang, Z. J.; Dang, H. X. *Mater. Lett.* **2005**, *59*, 3119.
(5) Hardacre, C.; Holbrey, J. D.; McMath, S. E. J.; Bowron, D. T.; Soper, A. K. *J. Chem. Phys.* **2003**, *118*, 273.
(6) Katayanagi, H.; Hayashi, S.; Hamaguchi, H. O.; Nishikawa, K. *Chem. Phys. Lett.* **2004**, *392*, 460.
(7) Xu, W.; Cooper, E. I.; Angell, C. A. *J. Phys. Chem. B* **2003**, *107*, 6170.
(8) Antony, J. H.; Mertens, D.; Dolle, A.; Wasserscheid, P.; Carper, W. R. *ChemPhysChem* **2003**, *4*, 588
(9) Shirota, H.; Castner, E. W. J. *J. Phys. Chem. A* **2005**, *109*, 9388.
(10) Naoki Ito, W. H.; Richert, R. *J. Phys. Chem. B* **2006**, *110*, 4371.
(11) Triolo, A.; Russina, O.; Hardacre, C.; Nieuwenhuyzen, M.; Gonzalez, M. A.; Grimm, H. *J. Phys. Chem. B* **2005**, *109*, 22061.
(12) Triolo, A.; Russina, O.; Arrighi, V.; Juranyi, F.; Janssen, S.; Gordon, C. M. *J. Chem. Phys.* **2003**, *119*, 8549.
(13) Urahata, S. M.; Ribeiro, M. C. C. *J. Chem. Phys.* **2005**, *122*, 024511 ~2005.
(14) McMorrow, D.; Lotshaw, W. T.; Kenney-Wallace, G. A. *IEEE J. Quantum Elec.* **1988**, *24*, 443.
(15) Hinze, G.; Brace, D.; Gottke, S. D.; Fayer, M. D. *Phys. Rev. Lett.* **2000**, *84*, 2437.
(16) Boon, P.; Yip, S. *Molecular Hydrodynamics*; McGraw-Hill: New York, 1980.
(17) Torre, R.; Bartolini, P.; Pick, R. M. *Phys. Rev. E: Stat. Phys., Plasmas, Fluids, Relat. Interdiscip. Top.* **1998**, *57*, 1912.
(18) Cang, H.; Li, J.; Andersen, H. C.; Fayer, M. D. *J. Chem. Phys.* **2005**, *123*, 064508.
(19) Cang, H.; Li, J.; Novikov, V. N.; Fayer, M. D. *J. Chem. Phys.* **2003**, *118*, 9303.
(20) Hinze, G.; Brace, D. D.; Gottke, S. D.; Fayer, M. D. *J. Chem. Phys.* **2000**, *113*, 3723.
(21) Gottke, S. D.; Brace, D. D.; Hinze, G.; Fayer, M. D. *J. Phys. Chem. B* **2001**, *105*, 238.
(22) Brace, D.; Gottke, S. D.; Cang, H.; Fayer, M. D. *J. Chem. Phys.* **2002**, *116*, 1598.
(23) Steffen, W.; Patkowski, A.; Meier, G.; Fischer, E. W. *J. Chem. Phys.* **1992**, *96*, 4171.
(24) Comez, L.; Corezzi, S.; Fioretto, D.; Kriegs, H.; Best, A.; Steffen, W. *Phys. Rev. E: Stat. Phys., Plasmas, Fluids, Relat. Interdiscip. Top.* **2004**, *70*, 011504/1.
(25) Patkowski, A.; Lopes, M. M.; Fischer, E. W. *J. Chem. Phys.* **2003**, *119*, 1579.
(26) Götze, W.; Sperl, M. *Phys. Rev. Lett.* **2004**, *92*, 105701.
(27) Götze, W. *Liquids, Freezing and Glass Transition*; Elsevier Science Publishers: Amsterdam, 1989.
(28) Götze, W.; Sjögren, L. *Rep. Prog. Phys.* **1992**, *55*, 241.
(29) Cang, H.; Novikov, V. N.; Fayer, M. D. *Phys. Rev. Lett.* **2003**, *90*, 197401(4).
(30) Cang, H.; Li, J.; Fayer, M. D. *J. Chem. Phys.* **2003**, *119*, 13017.
(31) Kai, Y.; Kinoshita, S.; Yamaguchi, M.; Yagi, T. *J. Mol. Liquids* **1995**, *65−6*, 413.
(32) Yan, Y. X.; Nelson, K. A. *J. Chem. Phys.* **1987**, *87*, 6240.
(33) Yan, Y. X.; Nelson, K. A. *J. Chem. Phys.* **1987**, *87*, 6257.
(34) Deeg, F. W.; Stankus, J. J.; Greenfield, S. R.; Newell, V. J.; Fayer, M. D. *J. Chem. Phys.* **1989**, *90*, 6893.

(35) Yan, Y. X.; Cheng, L. G.; Nelson, K. A. *Adv. Infrared Raman Spectrosc.* **1987**, *16*, 299.
(36) Gottke, S. D.; Brace, D. D.; Cang, H.; Bagchi, B.; Fayer, M. D. *J. Chem. Phys.* **2002**, *116*, 360.
(37) Cang, H.; Novikov, V. N.; Fayer, M. D. *J. Chem. Phys.* **2003**, *118*, 2800.
(38) Götze, W. *J. Phys. Condens. Matter* **1990**, *2*, 8485.
(39) Bartsch, E. *Transp. Theory Stat. Phys.* **1995**, *24*, 1125.
(40) Wiedersich, J.; Surovtsev, N. V.; Rössler, E. *J. Chem. Phys.* **2000**, *113*, 1143.
(41) Steffen, W.; Patkowski, A.; Gläser, H.; Meier, G.; Fischer, E. W. *Phys. Rev. E: Stat. Phys., Plasmas, Fluids, Relat. Interdiscip. Top.* **1994**, *49*, 2992.
(42) Götze, W.; Sjögren, L. *J. Phys. C: Solid State Phys.* **1988**, *21*, 3407.
(43) Sokolov, A. P.; Kisliuk, A.; Novikov, V. N.; Ngai, K. *Phys. Rev. B: Condens. Matter Mater. Phys.* **2001**, *63*, 172204.
(44) Ngai, K. L. *J. Chem. Phys.* **1999**, *110*, 10576.
(45) Kisliuk, A.; Novikov, V. N.; Sokolov, A. P. *J. Polym. Sci., Part B: Polym. Phys.* **2002**, *40*, 201.
(46) Gainaru, C.; Rivera, A.; Putselyk, S.; Eska, G.; Rössler, E. A. *Phys. Rev. B: Condens. Matter Mater. Phys.* **2005**, *72*, 174203.
(47) Bhattacharyya, S. M.; Bagchi, B.; Wolynes, P. G. *Phys. Rev. E: Stat. Phys., Plasmas, Fluids, Relat. Interdiscip. Top.* **2005**, *72*, 031509.
(48) Sjögren, L. *Phys. Rev. A: At., Mol., Opt. Phys.* **1986**, *33*, 1254.
(49) Li, J.; Cang, H.; Andersen, H. C.; Fayer, M. D. *J. Chem. Phys.* **2006**, *124*, 014902.
(50) Duval, E.; Mermet, A.; Le Parc, R.; Champagnon, B. *Philos. Mag.* **2004**, *84*, 1433.
(51) Ramos, M. A.; Talón, C.; Jiménez-Riobóo, R. J.; Vieira, S. *J. Phys.: Condens. Matt.* **2003**, *15*, S1007−S1018.
(52) Franosch, T.; Götze, W.; Mayr, M. R.; Singh, A. P. *Phys. Rev. E: Stat. Phys., Plasmas, Fluids, Relat. Interdiscip. Top.* **1997**, *55*, 3183.
(53) Li, Y.; Yu, P.; Bai, H. Y. *Appl. Phys. Lett.* **2005**, *86*, 231909.
(54) Yamamuro, O.; Minamimoto, Y.; Inamura, Y.; Hayashi, S.; Hamaguchi, H. *Chem. Phys. Lett.* **2006**, *423*, 371.